Quaternary International 397 (2016) 541–554

Contents lists available at ScienceDirect

Quaternary International

journal homepage: www.elsevier.com/locate/quaint

Holocene geohazard events on the southern Izu Peninsula, central Japan

Akihisa Kitamura [a, *], Yoko Ohashi [a], Hidemi Ishibashi [a], Yosuke Miyairi [b], Yusuke Yokoyama [b], Ryoya Ikuta [a], Yasuhiro Ito [c], Masayuki Ikeda [a], Taketo Shimano [d]

[a] Institute of Geosciences, Shizuoka University, 836 Oya, Suruga-ku, Shizuoka, 422-8529, Japan
[b] Atmosphere and Ocean Research Institute, University of Tokyo, Chiba, 277-8564, Japan
[c] University Museum, University of Tokyo, Tokyo, 113-0033, Japan
[d] Graduate School of Environment and Disaster Research, Tokoha University, Shizuoka, 417-0801, Japan

ARTICLE INFO

Article history:
Available online 21 May 2015

Keywords:
Holocene
Izu Peninsula
Emerged sessile assemblages
^{14}C ages
Co-seismic uplift
Scoria layer

ABSTRACT

Faunal compositions and ^{14}C ages of emerged sessile assemblages at four sites in the southern part of Izu Peninsula, central Japan, indicate that co-seismic uplift occurred at 1256–950 BC, AD 1000–1270, AD 1430–1660, and AD 1506–1815. The data suggest that the stress field in the southern part of Izu Peninsula changed to its current north–south compression at ca. 3100 BP, and that the recurrence intervals for uplift-inducing earthquakes have become shorter during the last 1000 years. The main faults responsible for this seismicity appear to be located offshore from the south part of Izu Peninsula. This study also examined a 1-cm-thick scoria layer deposited between 6940 and 6810 cal BP in the south part of Izu Peninsula. The layer, which had not been previously examined petrographically, consists of scoria grains derived from Izu-Oshima volcano located 40 km east of the study area, rather than from volcanoes located on Izu Peninsula itself.

1. Introduction

The Japan islands are located at the boundaries of the Eurasian, North American, Pacific and Philippine Sea plates (Fig. 1a). Consequently, large earthquakes, tsunamis, and extensive volcanic activity have occurred in this region as a result of a long history of plate collision, which has caused frequent catastrophic events in the region. Most recently, a magnitude 9.0 earthquake occurred on 11 March 2011 in the Japan Trench off northeast Japan, causing a mega-tsunami that resulted in ~20,000 deaths. Numerous studies have since re-examined the available geologic evidence for large historical earthquakes and tsunamis in the region; these include events in the area of the Suruga, Nankai, and Sagami troughs, located off southwest and central (e.g., Abe and Shirai, 2013; Fujiwara et al., 2013; Kitamura et al., 2013a, b; Kitamura and Kobayashi, 2014a, b). The Philippine Sea (PHS) plate is subducting beneath the Eurasian plate in both the Suruga and Nankai troughs, as well as beneath the North American plate in the Sagami Trough (Fig. 1). The AD 1854 Ansei-Tokai earthquake (M 8.4) and the AD 1923 great Kanto earthquake (M 7.9) occurred in the Suruga Trough and Sagami Trough, respectively (Fig. 1a, b), within the past 200 years.

Izu Peninsula, located at the northeastern edge of the Suruga Trough and the northwest edge of the Sagami Trough, occupies the northern tip of the PHS plate (Fig. 1a, b). Its northern margin represents a collision zone with central Japan, which is located on the Eurasian and North American plates (Sugimura, 1972; Somervill, 1978; Nakamura and Shimazaki, 1981).

The region's many active faults and the resulting seismicity indicate that active deformation is occurring on the Izu Peninsula (Sagiya, 1999). For example, the Tanna and Irozaki faults caused the AD 1930 North Izu earthquake (M 7.3) and the AD 1974 Off-Izu Peninsula earthquake (M 6.9), respectively (Fig. 1b). Izu Peninsula has experienced large earthquakes, tsunami and volcanic activity in the past, and is known to be tectonically active. For example, the coastal areas of the peninsula were attacked by large tsunamis generated by the AD 1854 Ansei-Tokai earthquake and the AD 1923 great Kanto earthquake (Usami, 1975; Hatori, 1976) (Fig. 1b). More than 100 monogenetic volcanoes are found within an area measuring 40 × 30 km, which covers the eastern part of Izu

* Corresponding author.
E-mail address: seakita@ipc.shizuoka.ac.jp (A. Kitamura).

http://dx.doi.org/10.1016/j.quaint.2015.04.021

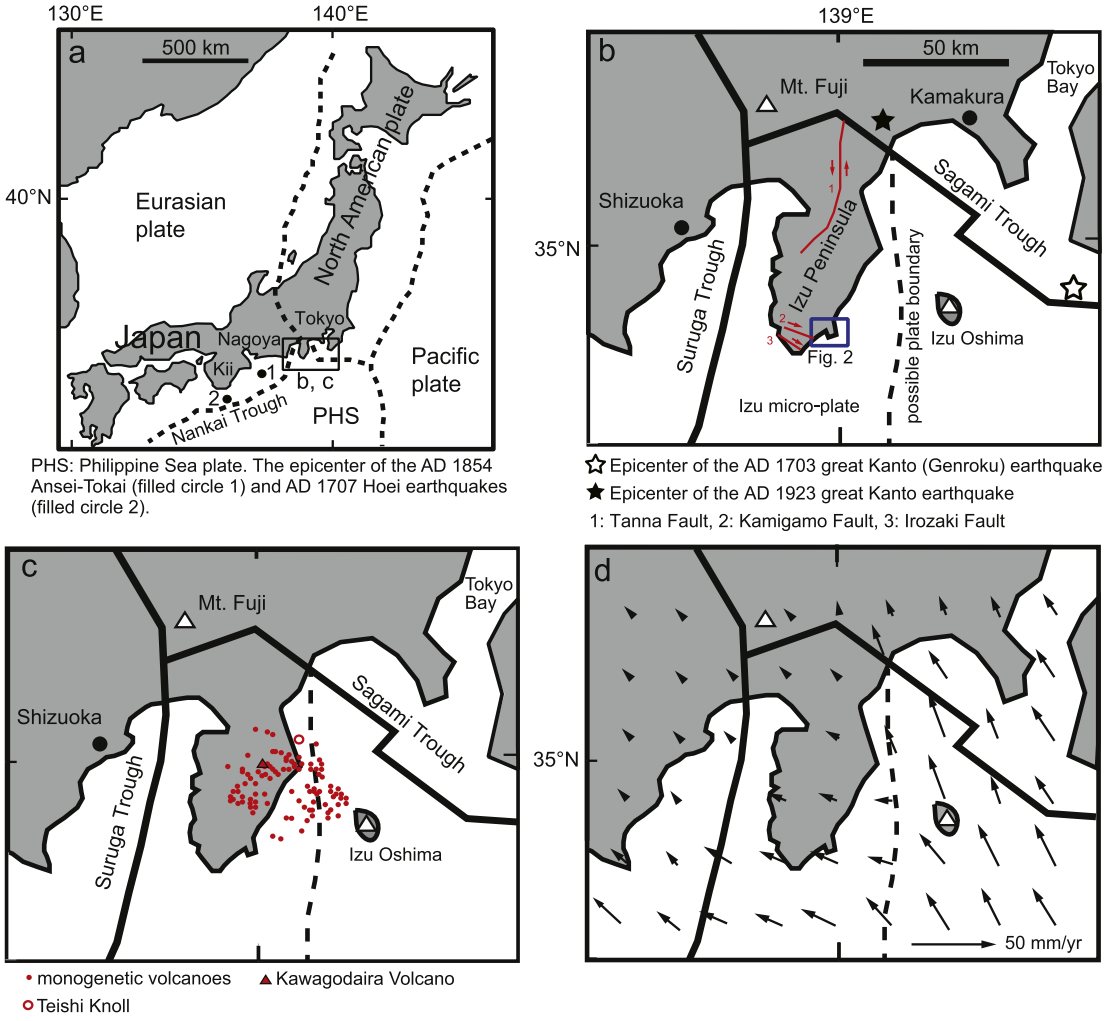

Fig. 1. Locality maps. (a) Japan Islands, showing plate boundaries, the location of Izu Peninsular, and epicenteral locations of the AD 1854 Ansei-Tokai and AD 1923 great Kanto earthquakes. (b) Locations of key active faults on Izu Peninsular. Possible plate boundary is after Nishimura et al. (2007). (c) Locations of monogenetic volcanoes on Izu Peninsular (Koyama and Umino, 1991; Notsu et al., 2014). (d) Arrows indicate the approximate directions of the sum of rigid block rotation and elastic deformation parts of the velocity field of the Kanto region predicted by the Euler pole of the best fit model in the central Japan block (CJP)-fixed reference frame (Nishimura et al., 2007).

Peninsula and the western part of Sagami Trough (Hamuro, 1985) (Fig. 1c); this area has been named the "Izu–Tobu Volcanoes" by the Japan Meteorological Agency (2005). The Teishi Knoll submarine volcano, which erupted on 1989, belongs to this group (Oshima et al., 1990, 1991). Similarity, the Kawagodaira Volcano erupted between 1210 and 1187 cal BC (95.4% confidence level) (Tani et al., 2013), resulting in pyroclastic flows in the surrounding area. The fine pumice from this volcano is widely distributed in the central and western parts of the Japanese mainland (Hamuro, 1977; Ikeya et al., 1990; Shimada, 2000).

Recent geodetic studies have proposed that the Izu microplate, which includes Izu Peninsular, moves separately from the rest of the PHS plate (Sagiya, 1999; Heki and Miyazaki, 2001; Nishimura et al., 2007), indicating that the Izu microplate is a region of concentrated deformation between Izu Peninsula and the main part of the PHS plate (Fig. 1d). Sagiya (1999) interpreted this tectonic movement as crustal deformation that is partitioned into left-lateral motion along a possible plate boundary located east of Izu Peninsula (the left-lateral Izu-Oshima Kinkai earthquake (M 6.5) occurred in this region in 1990; Abe and Okada, 1993) (Fig. 1b) and along the Zenisu Ridge, which is part of the suspected plate boundary (Nakanishi et al., 1994).

In this paper, we start by reviewing previous studies that have detailed Holocene geohazard events in the southern part of Izu Peninsula. We then provide new information on geohazard events, such as the co-seismic uplift history and volcanic activity in the area from middle–late Holocene. Co-seismic uplift history is reconstructed by faunal analysis and dating of emerged sessile assemblages. This method is commonly used in temperate areas (e.g., Shishikura et al., 2008; Iryu et al., 2009; Castilla et al., 2010; Scicchitano et al., 2011; Melnick et al., 2012). These data are also important to understand the evolution of the collision zone.

2. Study area

2.1. Crustal movements

Fukutomi (1935) reported abrupt uplifts of the southern end of Izu Peninsula based on emerged sessile assemblages. Ota et al. (1986) and Taguchi (1993) proposed that the area was subsiding up until 3000 BP. Ota et al. (1986) obtained non-calibrated ^{14}C ages of emerged shell fossils at Bentenjima, Shimoda, on the southern Izu Peninsular (Fig. 2); however, shell fossils can no longer be found at this site by human activities. The authors also obtained ^{14}C ages

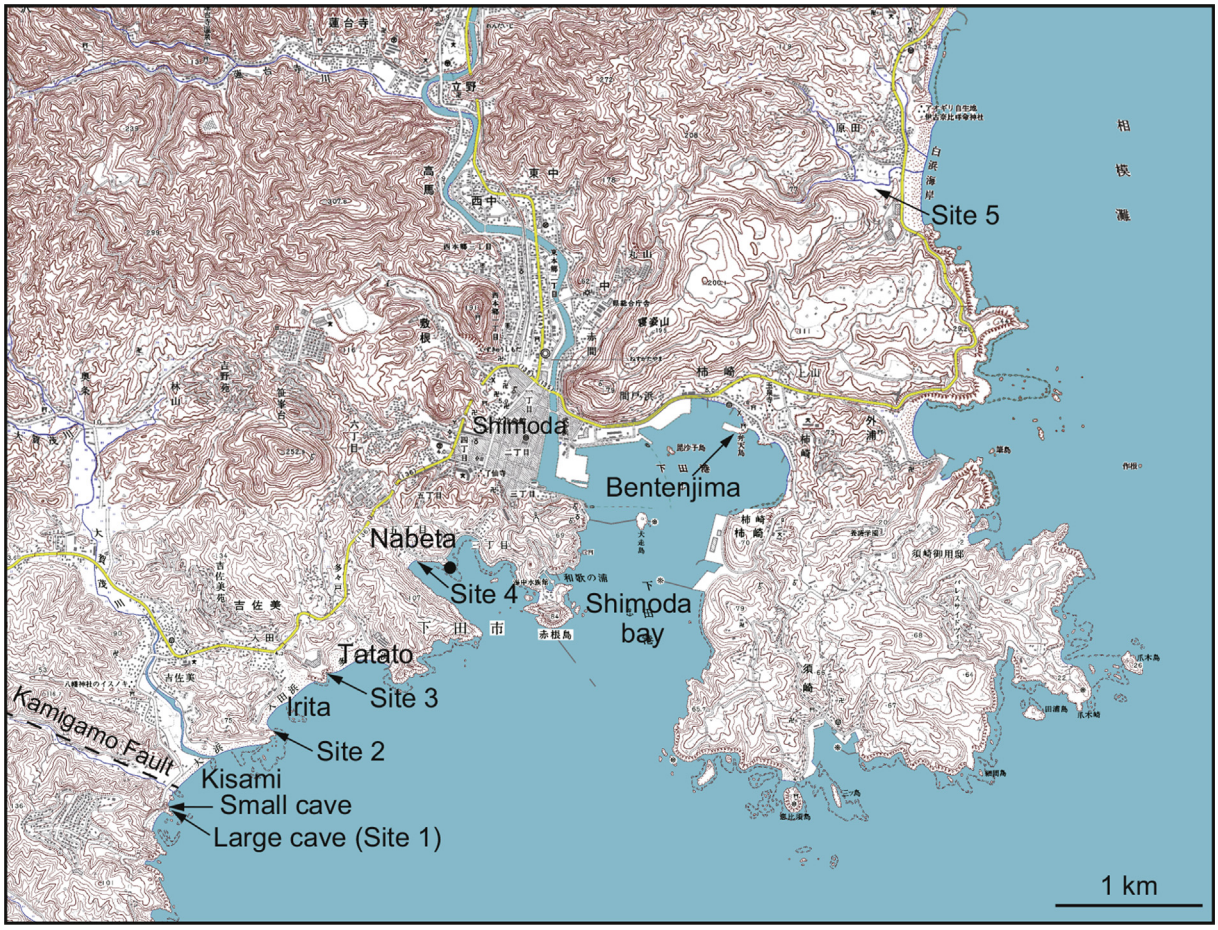

Fig. 2. Locations of the study areas on a 1:25,000 scale topographic map of the Shimoda and Kamiko Motojima districts (published by the Geospatial Information Authority of Japan). Closed circle is location of tsunami boulder caused by the Ansei-Tokai earthquake.

of shells from sessile assemblages in two coastal caves (hereafter referred to as the "large cave" and "small cave" in this text) on the Kisami coast, west Shimoda (Fig. 2). Based on these data, Ota et al. (1986) suggested that three uplift events took place during the past 3000 years, each probably caused by earthquakes.

Kitamura et al. (2014a) investigated the elevation distributions of emerged assemblages in the small cave (Fig. 2), and estimated the calendar ages of these assemblages using accelerator mass spectrometry (AMS) ^{14}C dating. The authors suggested that three episodes of coastal uplift have occurred in the area, during AD 570–820, AD 1000–1270, and AD 1430–1660, with uplift heights of 0.9–2.0 m, 0.3–0.8 m, and 1.9–2.2 m, respectively. Kitamura et al. (2013b) examined lithofacies and molluscs in sediment cores from a coastal plain at Minami Izu, located 7 km west of Shimoda. The results show that foreshore deposits younger than 4820–4590 cal BP are located at 2.0–2.6 m above mean sea level (amsl), indicating uplift by about ~2 m since 4820 cal BP.

2.2. Tsunami deposits

Kitamura et al. (2013b) conducted stratigraphic and paleo-enviromental research on Holocene deposits in the coastal lowlands of Minami Izu, located about 10 km southwest from Shimoda (Fig. 2). The Holocene sediments were deposited in a range of environments: coastal plain, shallow water, shoreface, backshore/dune, back marsh, and floodplain. However, no evidence for tsunami deposits was identified from the terrestrial deposits.

Kitamura and Kobayashi (2014b) reconstructed the Holocene sedimentary environment of Shimoda from sediment cores (Fig. 2), identifying four washover sand beds found in back-marsh deposits of coastal lowland areas in downtown Shimoda that are younger than 3500 cal BP. However, these sand beds were not identified as tsunami deposits.

Kitamura et al. (2014b) found emerged sessile assemblages on a boulder measuring 3.4 m long and estimated to weight 32 metric tons on a coastal plateau at Shimoda (Figs. 2 and 3). These assemblages consist mainly of small barnacles and tube worms, and distributed at 0.7–2.2 m amsl (Fig. 3c). They were not splashed by waves during high tide under fair-weather conditions. Based on AMS ^{14}C dating and the ecology of the emerged sessile assemblages, Kitamura et al. (2014b) concluded that the boulder was rolled by a tsunami associated with the AD 1854 Ansei-Tokai earthquake. This is the first report of a tsunami boulder caused by the Ansei-Tokai earthquake.

3. Site descriptions

This study examines emerged sessile assemblages at four sites on the west coast of Shimoda (Fig. 2); all four sites are coastal caves. Site 1 is a large cave on the Kisami coast (Fig. 4a, b) and has been described by Ishibashi et al. (1979) and Ota et al. (1986), who obtained non-calibrated ^{14}C ages of 2830 ± 90 BP and 2650 ± 80 BP for fossil shells found at an elevation of 2.3–2.7 m, and ages of 670 ± 75 BP and 645 ± 80 BP for fossil shells found at an elevation of

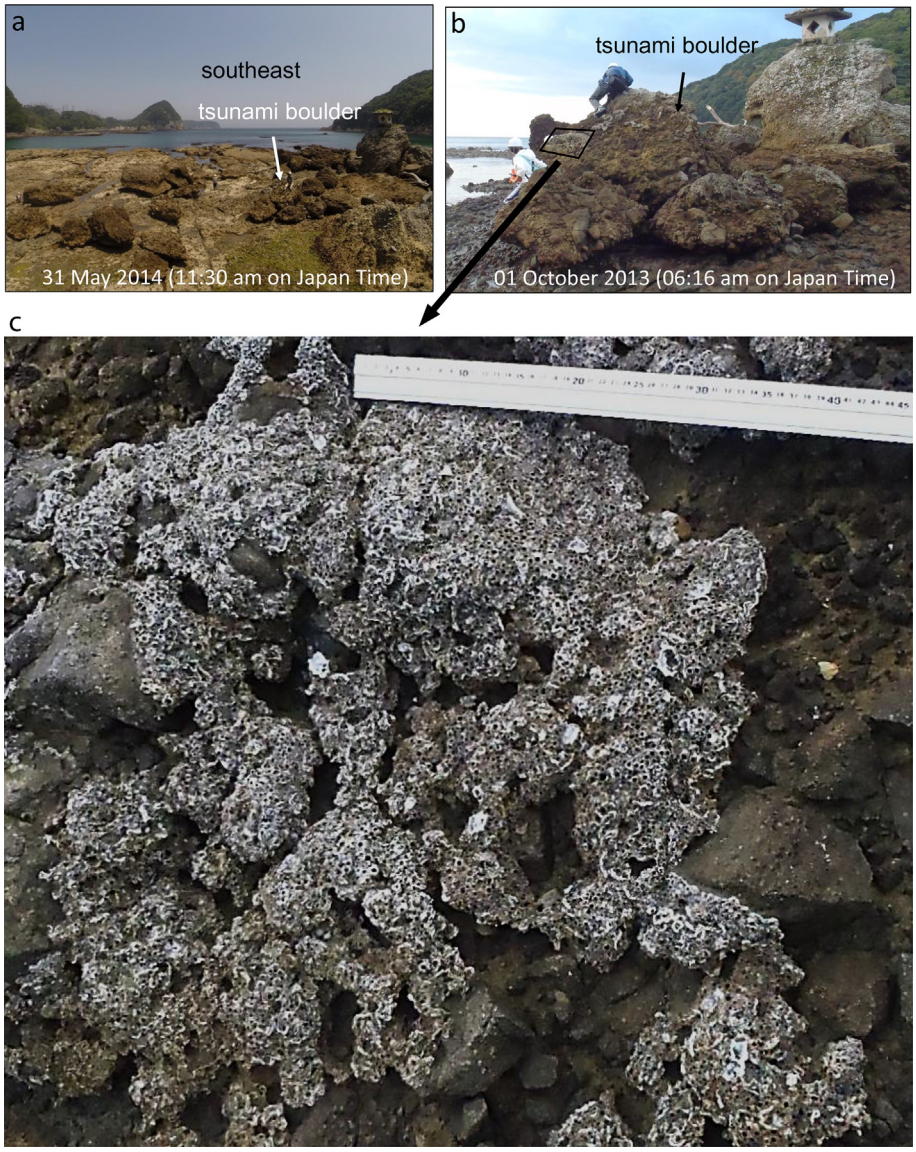

Fig. 3. Outcrop of a tsunami boulder on a wave-cut bench at Nabeta, Izu Peninsular. (a) Air photograph of the tsunami boulder. (b) Close-up of the tsunami boulder. (c) Well-preserved individuals of small barnacles on the tsunami boulder.

0.9–1.1 m amsl. The ^{14}C ages of 2830 ± 90 BP, 2650 ± 80 BP, 670 ± 75 BP, and 645 ± 80 BP were translated to calendar ages of BC 1235–777 (2σ), BC 991–589 (2σ), AD 1280–1527 (2σ), and 1294–1556 (2σ), respectively (Kitamura et al., 2014a). The length, width, and height of the cave are 63, 13, and 10 m, respectively (Fig. 4a, b), and the cave develops in Plio-Miocene tuffceous breccia of the Shirahama Group. The emerged sessile assemblages are found inside the cave at 37–50 m from the cave's entrance (Fig. 4c).

Site 2 is located at the base of a cliff on the western edge of the Irita coast (Figs. 2 and 5) and has been described in detail by Ota et al. (1986), who obtained a non-calibrated ^{14}C age of 950 ± 90 BP for fossil shells at elevations of 1.45–2.15 m amsl. The length, width, and height of the cave are 15, 7, and 5 m, respectively (Fig. 5a). This cave also develops in Plio-Miocene tuffceous brecchia of the Shirahama Group. The emerged sessile assemblages occur at the wall rocks at the cave's entrance (Fig. 5a, b, c). This study also found sessile assemblages, which are located at 0 m amsl and are usually covered by sand, on basement rocks in front of the cave's entrance (Fig. 5d).

Site 3 is a coastal cave located in a cliff on the western edge of Tatato coast (Figs. 2 and 6a, b). The base of the cave's entrance lies at ~2.5 m amsl, and the entrance is roughly 4 m high and 7 m wide. The cave is 16 m long and occurs in Plio-Miocene cross-laminated pumiceous tuff. We found many *in situ* individuals of the boring bivalve Pholadidae at the entrance of the cave at an elevation of 2.7 m amsl (Fig. 6c).

Site 4 is located at a small cliff on the Nabeta coast (Figs. 2 and 7a, b). The base of the coastal cave's entrance is ~1.4 m amsl, and the entrance is roughly 2 m high and 4 m wide. The cave is 5 m long and develops in Plio-Miocene cross-laminated pumiceous tuff. We found many *in situ* fossils of boring shells at an elevation of 1.4 m amsl in the entrance of the cave (Fig. 7c).

This study also examines the petrography of scoria found in sedimentary cores at site 5 by Kitamura and Kobayashi (2014b) (Fig. 2). This site is located in narrow wetlands between hills and sand dunes, and is ~2.50 m amsl. Kitamura and Kobayashi (2014b) studied an 8-m-long core and concluded that the sediments were deposited at the back marsh (Fig. 8). The scoria layer is located

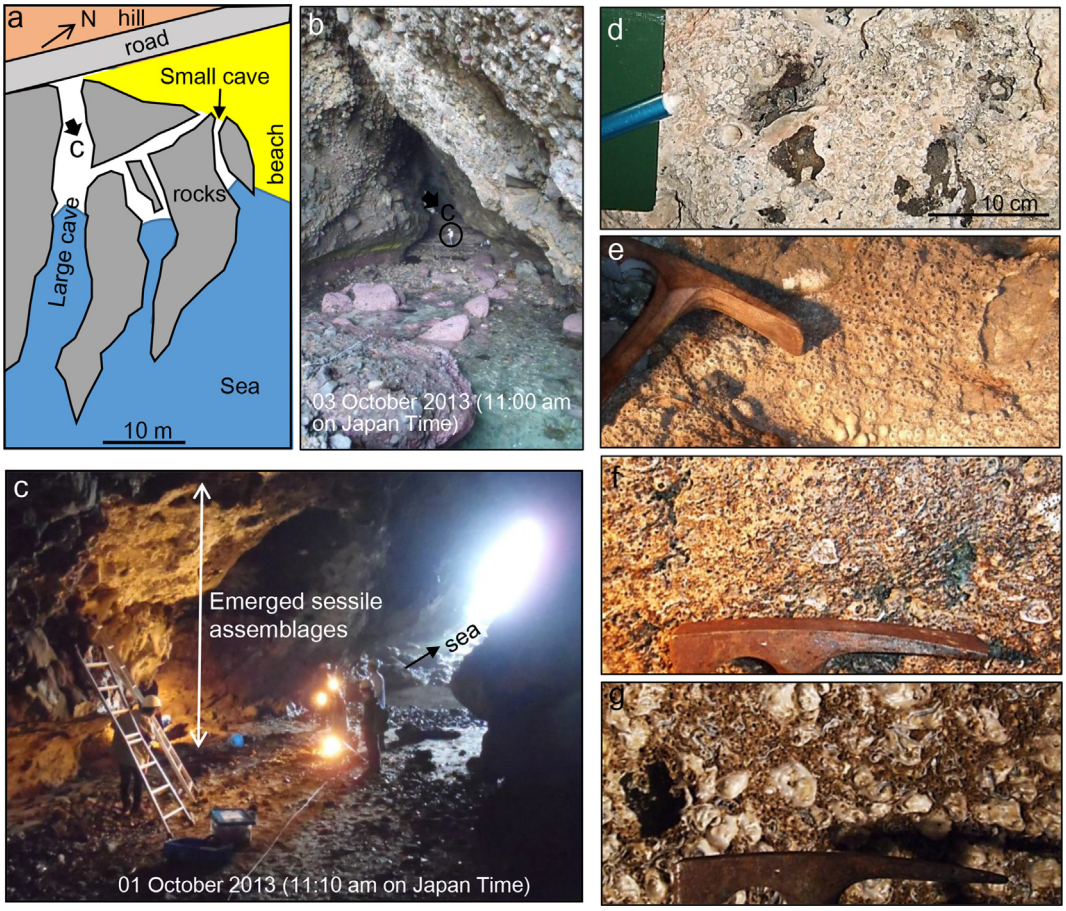

Fig. 4. (a) Simplified horizontal projection of the coastal caves at site 1. (b) Seaside entrance to the large cave. (c) Outcrop of emerged sessile assemblages. (d) Examples of *Tetraclitella chinensis* in Zone A. (e) Examples of *T. chinensis* in Zone B. (f) Co-occurrence of *T. chinensis*, and *Pomatoleios kraussii* in Zone C. (g) Examples of *Saccostrea kegaki* and *P. kraussii*. in Zone D.

at −1.28 m amsl, 0.66 m above the Kikai-Akahoya tephra (7303–7165 cal BP; Smith et al., 2013) (Fig. 8). The ^{14}C ages of leaves located just below and above the scoria layer are 6940–6760 cal BP and 7000–6810 cal BP, respectively. The depositional age of the scoria is therefore estimated to be within the interval 6940–6810 cal BP. Scoria grains are very fresh and angular, and measure up to 1 cm long. To our knowledge, no previous study has reported on a scoria layer from Izu Peninsular.

The coastline at the southern end of Izu Peninsula is characterized by a wave-dominated and microtidal regime, with a maximum tide range of 1.6 m during spring tide. In this study, the present mean sea level is based on tidal records at Bentenjima, Shimoda Bay. Based on leveling records from the period 1896–1968 (Danbara and Tsuchi, 1975), the study area appears to have subsided at a rate of ~0.6 mm/yr. Both the Irozaki and Kamigamo faults cross the study area and are WNW–ESE trending right-lateral faults (Murai and Kaneko, 1974) (Fig. 1b). The AD 1974 Off-Izu Peninsula earthquake caused an uplift of 0.1 m on the Irozaki fault (Danbara and Tsuchi, 1975).

4. Methods

Emerged sessile assemblages are exposed continuously at sites 1 and 2. Samples of the assemblages were collected at an average of 20 cm increments in elevation at both sites. At sites 3 and 4, we collected several individuals of well-preserved bivalves. Under laboratory conditions, specimens were cleaned with a micro-knife and then identified. Specimens were checked for the absence of secondary crystallization within cavities of shells, using a binocular microscope. We determined the radiocarbon ages of 40 boring shells and sessile organisms (including *S. kegaki*, barnacles, and calcareous tubes of *Pomatoleios kraussii*) using an accelerator mass spectrometry at University of Tokyo, Japan, and at Beta Analytic Inc., USA (Table 1). Ages were then translated onto a calendar timescale using the program OxCal4.1 (Bronk Ramsey, 2009), based on comparisons with IntCal13 data (Reimer et al., 2013) after applying a local correction for the Shimoda area of $\Delta R = 109 \pm 60$ (Yoneda et al., 2000).

Bulk rock major element compositions were measured using a Rigaku RIX 2100 X-ray fluorescence spectrometer at the Graduate School of Environment and Disaster Research, Tokoha University, Japan, employing the glass bead method. A glass bead is created by dissolving a rock powder sample in molten anhydrous lithium tetra-borate flux at a ratio of 1.0 g sample to 5.0 g flux (Sano, 2003). Two grains of scoria, ~1 cm in diameter and sampled from the drill core, were crushed and mixed to make a homogeneous powder sample for XRF analysis.

Back-scattered electron (BSE) images of the scoria were acquired with a scanning electron microscope (SEM) at the Department of Geoscience, Graduate School of Science, Shizuoka University, Japan. The volume fraction of bubbles in the scoria was measured from BSE images by counting the numbers of pixels in the bubble areas in the image. Major element compositions of silicate glass were analyzed using a JXA-8800R EPMA at Earthquake Research

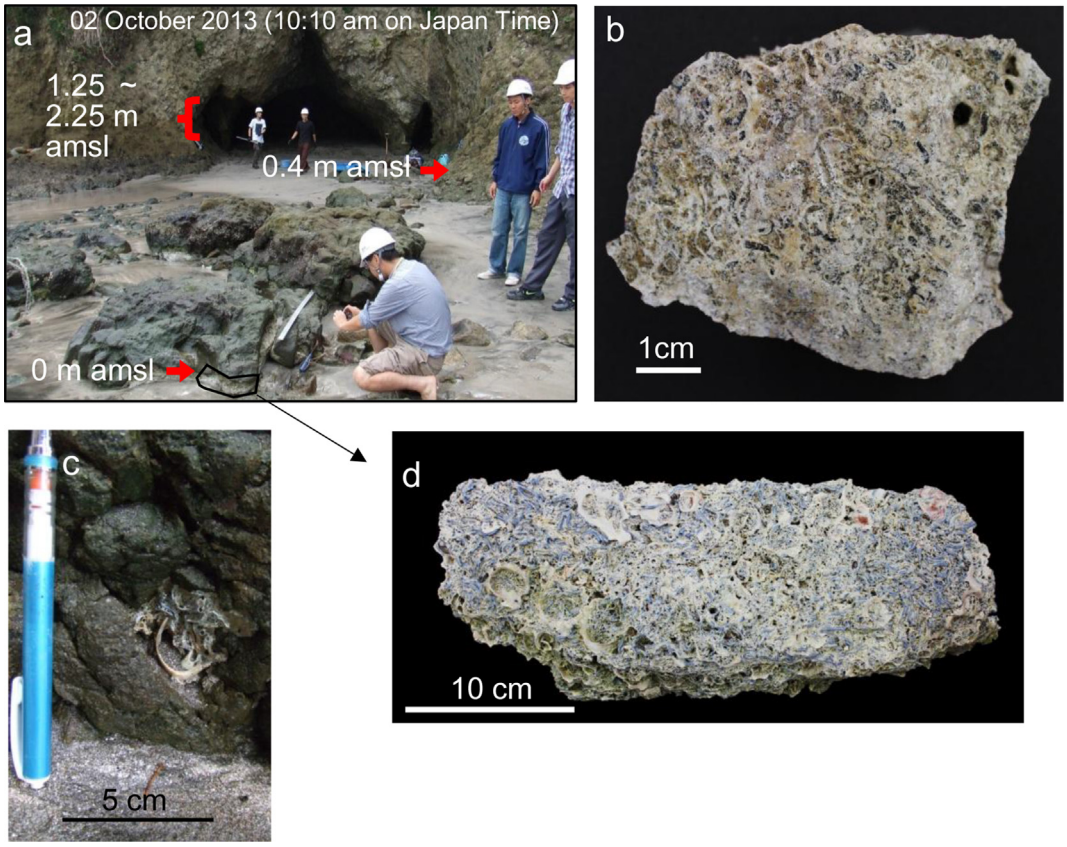

Fig. 5. (a) Photograph showing the coastal cave at site 2. (b) Abraded individualewes of *P. kraussii* and *Tetraclitella* sp. at 1.25 m amsl. (c) A small cluster of very fresh *P. kraussii* at 0.41 m amsl. (d) Co-occurrence of fresh *P. kraussii* and *S. kegaki* at 0 m amsl.

Institute, the University of Tokyo, Japan, using an accelerating voltage of 15 kV, a beam current of 12 nA, and a beam diameter of 10 μm. The refractive index of glass shards were analyzed by Kyoto Fission Track Inc., Japan using method by Danhara et al. (1992).

5. Results

5.1. Emerged sessile assemblages

At Site 1, the emerged sessile assemblages occur continuously between 0.14 and 3.40 m amsl (Fig. 4c) and are up to 2 cm thick. We did not observe any layered structure composed of multiple vertical layers within the assemblages. The assemblages are divided into four zones, as follows.

Zone A occurs between elevations of 2.44 and 3.40 m amsl and consists of strongly abraded *Tetraclitella chinensis* (Fig. 4d). *P. kraussii* are rarely observed in the lower portion of Zone A. Zone B occurs between elevations of 1.75 and 2.44 m amsl and is dominated by abraded *T. chinensis* (Fig. 4e). Zone C occupies elevations between 0.94 and 1.75 m amsl and consists of fresh *T. chinensis* that are associated with *P. kraussii* (Fig. 4f). Zone D occupies elevations between 0.14 and 0.94 m amsl and is characterized by the co-occurrence of fresh shells of *S. kegaki*, *P. kraussii*, and *T. chinensis* (Fig. 4g).

Table 1 lists the radiocarbon ages obtained from the sampled bivalves and barnacles, which are plotted in Fig. 9. In Zone A, all ^{14}C ages (2σ) fall within 1500–950 BC, except for one significantly older example estimated at between 2860 BC and 2470 BC. The ^{14}C age distribution in Zone B exhibits a wider range from 1570 BC to AD 1112. All ^{14}C ages in Zones C and D fall within AD 1066–1494 and AD 1454–1950, respectively.

At site 2, the emerged sessile assemblages outcrop continuously between 1.25 and 2.25 m amsl and are up to 2 cm thick. We did not observe any layered structure composed of several vertical layers within the assemblages. The assemblages consist of abraded *P. kraussii* and *Tetraclitella* sp. (Fig. 5b). There is a small cluster (~10 cm^2) of very fresh *P. kraussii* at 0.41 m amsl (Fig. 5c). Sessile assemblages at 0 m amsl consist of fresh *P. kraussii* and *S. kegaki* (Fig. 5d). The ^{14}C ages of specimens from between 1.25 and 2.25 m amsl vary from AD 0–1430. The ages of specimens at 0.41 m and 0 m amsl fall within AD 1310–1890 (Fig. 9).

This study analyzed three individuals of the boring bivalve Pholadidae found *in situ* at an elevation of 2.70 m amsl from the coastal cave at site 3 (Fig. 6c). Their ^{14}C ages are similar to each other and fall within BC 1466–1250 (Fig. 9). We obtained four specimens of boring shells of *Jouannetia* and *Zirfaea* found *in situ* at an elevation of 1.4 m amsl from the coastal cave at site 4 (Fig. 7c). All ^{14}C ages fall within AD 839–1180 (Fig. 9).

5.2. Scoria

Fig. 10 shows a back-scattered electron image of the scoria. It is aphyric, glassy, and highly vesicular. Bubbles show an isometric round shape with a volume fraction of ~0.65. The solid part of the scoria is mainly silicate glass with microlites of plagioclase, pigionite, and augite. Plagioclase is tabular and 70 μm long. Pigeonite and augite crystals are euhedral–subhedral, columnar, and <10 μm.

The bulk-rock major element composition of the scoria is shown in Table 2. The scoria is classified as basaltic andesite according to the scheme of Le Mitre (2002), with an SiO_2 content of 53.8 wt% and a (Na_2O + K_2O) content of 2.47 wt%. Silicate glass in the scoria is

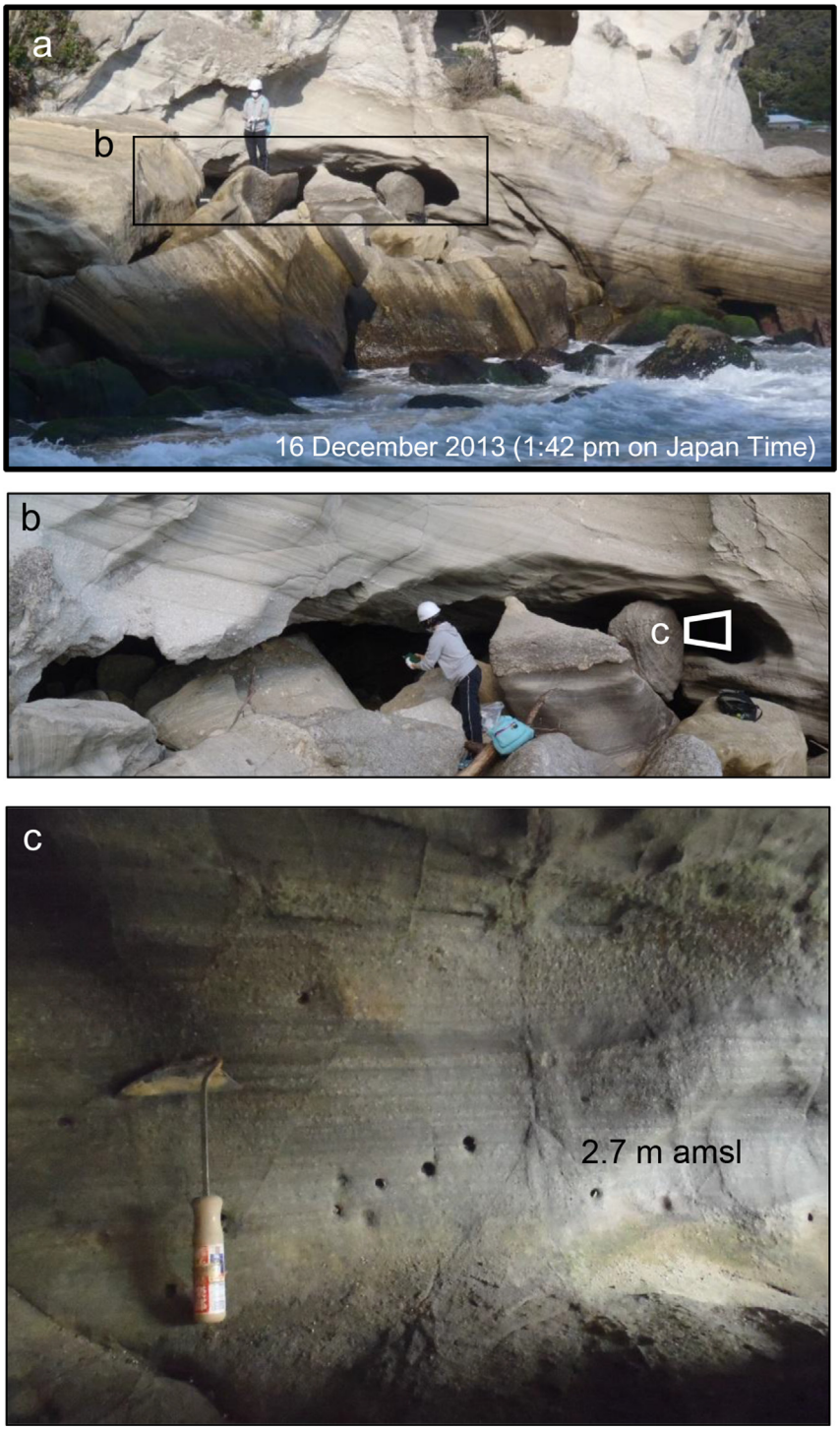

Fig. 6. (a) Photograph showing the coastal cave at site 3. (b) Close-up of the entrance of the coastal cave. (c) Occurrence of boring shells.

chemically homogeneous and has a more evolved composition than the bulk scoria, with higher SiO_2, TiO_2, and K_2O contents, and a higher $\underline{FeO^*}/MgO$ ratio [where FeO^* is total iron oxide content calculated as FeO] (Table 2). This can be attributed to the crystallization of microlites. The mass fraction of glass in the scoria is estimated by the ratio of K_2O content in glass to the ratio in bulk rock, K_2O^{glass}/K_2O^{bulk}, and assumes negligible K_2O content in both plagioclase and pyroxene. The ratio of 1.06 indicates that the mass fraction of silicate glass is ~0.94. The refractive index of glass shards ranges from 1.5925 to 1.5985, with a peak around 1.5955–1.5965 (Fig. 8).

6. Discussion

6.1. Coseismic uplifts

Fig. 9 illustrates our ^{14}C data plotted against the data of Kitamura et al. (2014a). The figure shows that numerous emerged

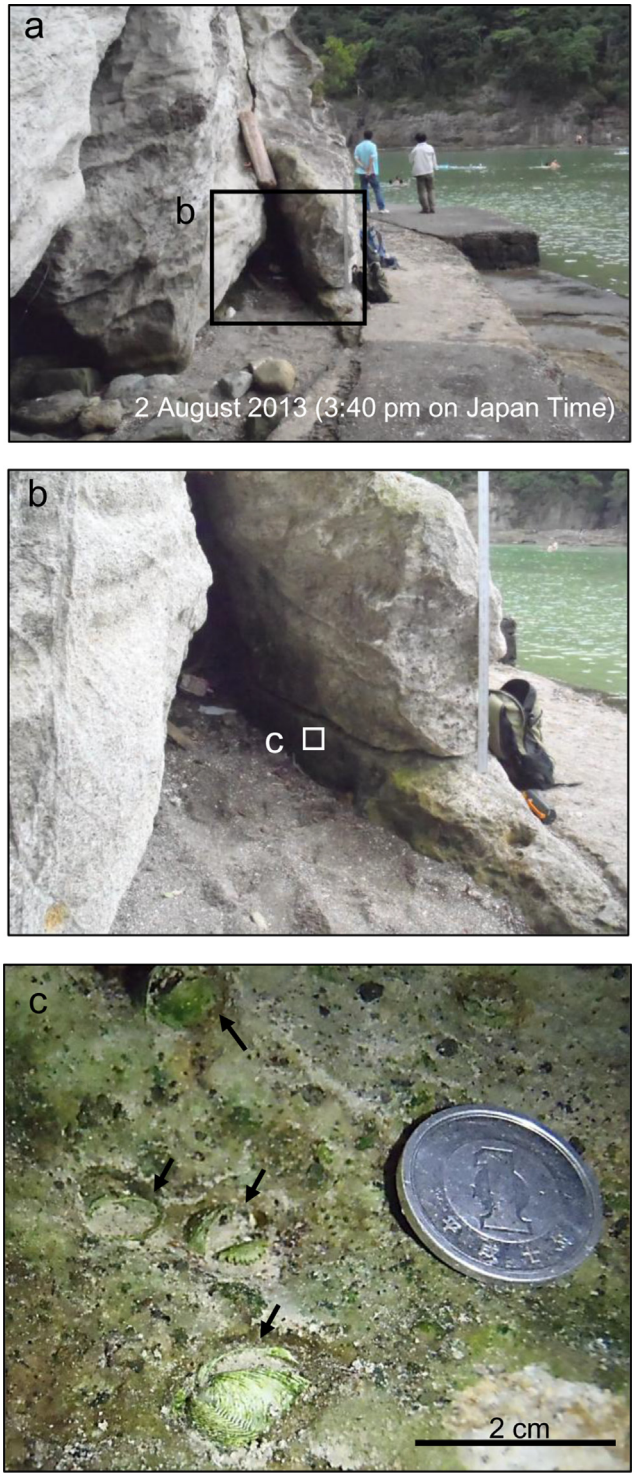

Fig. 7. (a) Photograph showing the coastal cave at site 4. (b) Close-up of the entrance of the coastal cave. (c) Occurrence of boring shells.

sessile assemblages are distributed above the upper limit of the vertical distribution of living species in the study area.

At site 1, Zone A (elevations of 2.44 and 3.40 m amsl) consists of the barnacle *T. chinensis*. According Yamaguchi and Hisatsune (2006), *T. chinensis* lives within the intertidal zone from −0.8 to 0.8 m amsl. Given that the top of Zone A (3.40 m amsl), which consists of *T. chinensis*, corresponds to the upper limit of the intertidal zone, the zone must have experienced a minimum uplift of 2.6 m since active growth ended in this zone. Similarly, the elevation of Zone B (1.75–2.44 m amsl) suggests a minimum uplift of 1.64 m since active growth ceased. Zone C occupies elevations between 0.94 and 1.75 m and consists of mixture of *T. chinensis*, and *P. kraussii*. Kitamura et al. (2014a) reported that the upper elevation limit of *P. kraussii* is 0.1–0.2 m amsl on the coastline at Bentenjima and Irita (Fig. 2). As the top of zone C corresponds to the upper limit of *P. kraussii*, the total uplift is estimated to be at least 1.55 m since active growth ended in this zone. Zone D occurs at elevations of 0.14–0.94 m amsl and is characterized by the co-occurrence of fresh shells of *S. kegaki*, *P. kraussii*, and *T. chinensis*. *S. kegaki* and *P. kraussii* co-occur up to elevations of ~0.2 m amsl at Shimoda (Kitamura et al., 2014a). The elevation of the top of Zone D (0.94 m amsl) therefore suggests a minimum uplift of 0.74 m has occurred since active growth ceased in this zone. The elevations of these zones indicate that the growth of sessile marine organisms ceased at least four times, each possibly caused by an abrupt uplift event.

Kitamura et al. (2014a) examined the faunal compositions and ^{14}C dating of the emerged assemblages in the small cave, located 20 m east from the large cave (Fig. 2a). The emerged assemblages could be divided into five zones: Zone I (2.7–3.5 m amsl), II (2.35–2.7 m amsl), III (2.0–2.35 m amsl), IV (1.6–2.0 m amsl) and V (1.0–1.60 m amsl) (Fig. 9). The termination of the growth of the assemblages took place during AD 570–820 (Zone I), AD 1000–1270 (Zones II and III), and AD 1430–1660 (Zones IV and V), respectively. The authors suggested that these terminations were caused by three episodes of coastal uplift, with uplift amounts of 0.9–2.0 m, 0.3–0.8 m, and 1.9–2.2 m, respectively.

Comparison of the elevations and ^{14}C age distributions of faunal zones between the large and small caves suggests that Zones B and C correspond to Zones II–III and Zones IV–V, respectively (Fig. 4). The small discrepancy in the elevation of these zones is explained by differences in the elevation of the swash zone; this is related to the differences in the topographic features between these two caves (Fig. 4a). Our data confirm Kitamura et al. (2014a) hypothesis that coastal uplifts occurred at AD 1000–1270 and AD 1430–1660.

Zone A corresponds to Zone I in terms of the elevation. Since Zone I consists of a very hard massive shell crust with a strong erosional surface, Kitamura et al. (2014a) obtained ^{14}C ages form the bivalve *Hormomya mutabilis* (AD 480–750), *Lasaea undulate* (AD 570–820), and *Lithophaga curta* (1420–1080 BC) (Fig. 9). They did not consider any surface-dwelling sessile organisms such as barnacles, oysters, or tube worms. However, the present study obtained five ^{14}C age estimates for barnacles and tube worms. Although the specimens are abraded (Fig. 4d), their state of preservation is much better in Zone A than in Zone I. This discrepancy arises because the wave energy is weaker at Zone A than at Zone I, due to Zone A being located farther from the cave entrance (37 m) than Zone I (5–6 m). From our data, we interpret that rapid uplift occurred between 1256 BC (2σ older limit of age of Sample KSM121) and 950 BC (2σ younger limit of age of Sample KSM151), and caused the cessation of activity in Zones A and I. In addition, two molluscs specimens with significantly younger ages in Zone I may indicate that the emerged assemblages fell into the intertidal zone during AD 570–750. Given that the rate of subsidence has been the same as that between 1896 and 1968 (0.6 mm/yr; Danbara and Tsuchi, 1975), the subsidence is estimated to be 0.91–1.20 m. The lack of recolonization of sessile organisms at the surface of Zones A and I may be explained by the presence of unsuitable environments for sessile invertebrates due to excessive wave strength.

This study obtained ^{14}C ages for four specimens from Zone D (0.14–0.94 m amsl) that partly overlaps an intertidal zone. Among these ages, the age of *P. kraussii* (sample KSM021, 0.64 m amsl) (AD 1506–1815), whose upper limit of occurrence is 0.1–0.2 m amsl,

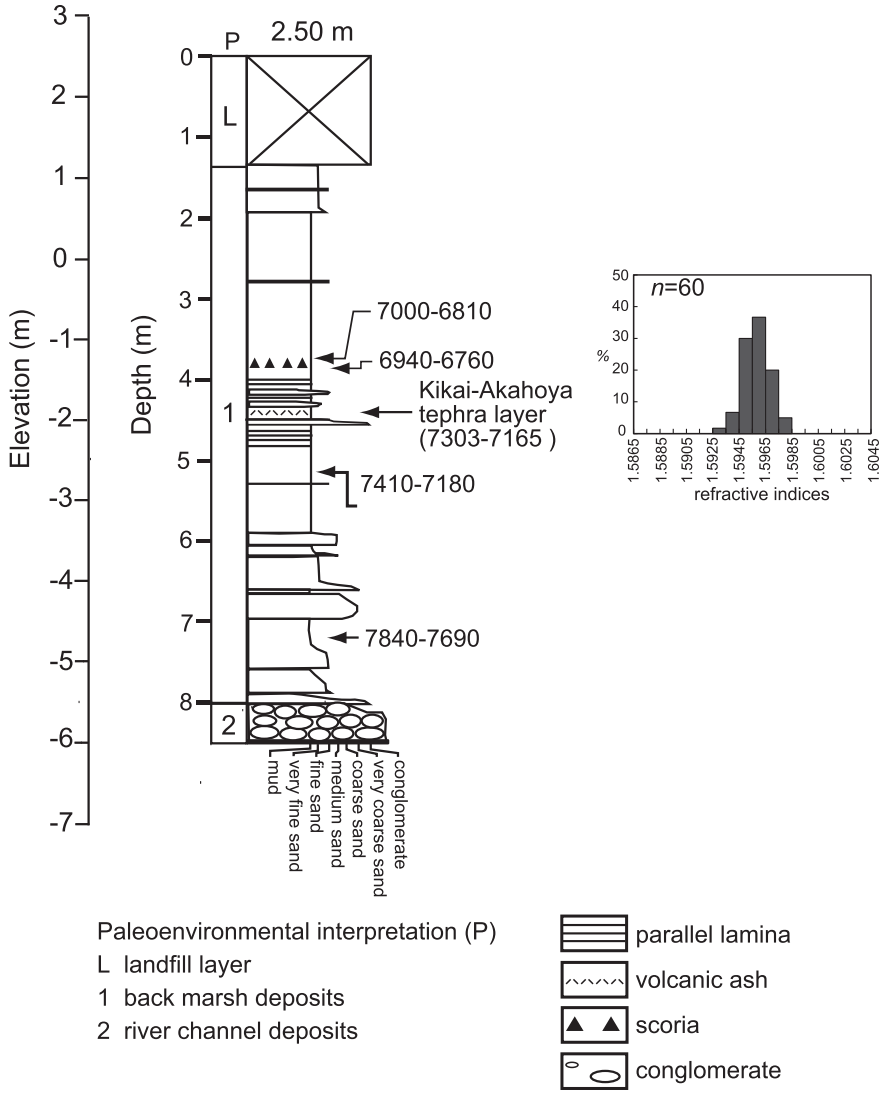

Fig. 8. (a) Columnar section at site 5, showing the stratigraphic position of the scoria layer and histogram of refractive indices of the scoria.

provides a reliable estimate for when activity associated with uplift in this zone ended.

In summary, the results suggest that four coastal uplift events occurred at 1256–950 BC, AD 1000–1270, AD 1430–1660 and AD 1506–1815; hereafter, these are referred to as Uplifts 1, 2, 3, and 4 respectively. Historical documents show that a large earthquake took place around the southern Izu Peninsular at AD 1729 (Usami, 1975). This earthquake may be related to Uplift 4.

We also estimated the total uplift experienced during Uplifts 1–4 using uplift amounts obtained from the emerged assemblages at site 1 along with inter-seismic subsidence rates and uplift resulting from the AD 1974 Off-Izu Peninsula earthquake. Although other earthquakes may have generated vertical crustal movements in the study area, co-seismic deformation lies outside the scope of this study. From mean inter-seismic subsidence rate (0.6 mm/yr) and 0.1 m uplift at AD 1974 Off-Izu Peninsular earthquake, uplifts are estimated to have been 1.67–2.97 m at Uplift 1, 0.01–0.67 m at Uplift 2, 0.72–1.04 m at Uplift 3, and 0.76–0.94 m at Uplift 4.

The emerged sessile assemblages found at site 2 yield ages of AD 0–1430. They outcrop continuously between 1.25 and 2.25 m amsl and include *P. kraussii* and *Tetraclitella* sp. Since the upper limit of the assemblages (2.25 m amsl) represents the upper limit of the distribution of living *P. kraussii* (0.2 m amsl), the total uplift is estimated to be at least 2.05 m since active growth last occurred at the site. Given that the estimated ages of specimens IRD81, 82, 91 and 92 (1.85–2.05 m amsl) are close to those of Zone B at site 1 (Fig. 9), their positions may be compared with Uplifts 2, 3 and 4. For the same reason, the position of specimen IRD51 at 1.25 m a result of Uplifts 3 and 4. A small cluster of very well-preserved *P. kraussii* (IRD42; AD 1340–1660) occurs at 0.41 m amsl, indicating a minimum uplift of 0.21 m since active growth last occurred. Given that the age of the specimen is matched with that of Zone D, its position seems likely to be related to Uplift 4. Conversely, since the distribution sub-fossils of *P. kraussii* and *S. kegaki* at 0 m amsl occurred within their living environment, their growth was probably stopped by being buried under sand.

As boring shells cannot inhabit the area above the upper limit of the intertidal zone (0.8 m amsl), the distribution of boring shells at sites 3 and 4 suggests uplifts of at least 1.9 m and 0.6 m, respectively, since the time of active growth of these specimens. On the

Table 1
Results of ^{14}C dating.

Sample name	Site	Height (m)	Zone	Laboratory number	Materials	Conventional ^{14}C age (yr BP)	Calibrated age (1σ)	Calibrated age (2σ)
KSM011	1	0.14	4	080803-2	*Saccostrea kegaki*	664 ± 39	Cal AD 1697–1811	Cal AD 1667–1890
KSM012	1	0.14	4	080803-4	*Saccostrea kegaki*	633 ± 63	Cal AD 1703–1871	Cal AD 1685-modern
KSM021	1	0.64	4	080704-1	*Pomatoleios kraussii*	762 ± 63	Cal AD 1555–1701	Cal AD 1506–1815
KSM022	1	0.64	4	080704-2	*Tetraclitella chinensis*	902 ± 34	Cal AD1470–1541	Cal AD 1454–1618
KSM031	1	1.14	3	080730-2	*Tetraclitella chinensis*	1051 ± 65	Cal AD 1349–1451	Cal AD 1302–1494
KSM032	1	1.14	3	080730-3	*Pomatoleios kraussii*	1175 ± 67	Cal AD 1274–1390	Cal AD 1206–1432
KSM042	1	1.31	3	080730-4	*Hormomya mutabilis*	1297 ± 56	Cal AD 1170–1280	Cal AD 1077–1305
KSM052	1	1.49	3	080730-5	*Hormomya mutabilis*	1337 ± 33	Cal AD 1137–1235	Cal AD 1077–1265
KSM061	1	1.66	3	080806-1	*Pomatoleios kraussii*	1316 ± 56	Cal AD 1149 1272	Cal AD 1066–1293
KSM062	1	1.66	3	080803-4	*Hormomya mutabilis*	1410 ± 80	Cal AD 1020–1200	Cal AD 940–1280
KSM071	1	1.84	2	080704-0	*Tetraclitella chinensis*	1792 ± 25	Cal AD 673–730	Cal AD 659–773
KSM072	1	1.84	2	080704-1	*Tetraclitella chinensis*	2813 ± 75	Cal BC 580-350	Cal BC 740-290
KSM081	1	2.01	2	080704-015	*Tetraclitella chinensis*	1548 ± 22	Cal AD 930–1009	Cal AD 901–1030
KSM082	1	2.01	2	080704-2	*Hormomya mutabilis*	3323 ± 42	Cal BC1150-990	Cal BC 1210-930
KSM091	1	2.18	2	080704-025	*Tetraclitella chinensis*	1472 ± 20	Cal AD 1011–1061	Cal AD 983–1112
KSM092	1	2.18	2	080704-3	*Hormomya mutabilis*	3607 ± 49	Cal BC 1500-1370	Cal BC 1570-1290
KSM101	1	2.36	2	080704-035	*Hormomya mutabilis*	1626 ± 20	Cal AD 826–915	Cal AD 795–960
KSM111	1	2.53	1	080704-036	*Pomatoleios kraussii*	3572 ± 24	Cal BC 1437-1362	Cal BC 1473-1303
KSM121	1	2.70	1	080704-037	*Pomatoleios kraussii*	3360 ± 44	Cal BC 1194-1052	Cal BC 1256-985
KSM122	1	2.70	1	080704-4	*Tetraclitella chinensis*	4553 ± 73	Cal BC 2820-2560	Cal BC 2860-2470
KSM131	1	2.88	1	080710-1	*Tetraclitella chinensis*	3425 ± 82	Cal BC 1350-1090	Cal BC 1420-980
KSM141	1	3.05	1	080710-2	*Tetraclitella chinensis*	3516 ± 42	Cal BC 1390-1270	Cal BC 1430-1200
KSM151	1	3.23	1	080710-3	*Tetraclitella chinensis*	3451 ± 99	Cal BC 1380-1110	Cal BC 1500-950
IRD11	2	0.00	–	080730-3	*Saccostrea kegaki*	741 ± 80	Cal AD 1560–1810	Cal AD1490–1890
IRD12	2	0.00	–	080730-4	*Pomatoleios kraussii*	901 ± 124	Cal AD 1430–1650	Cal AD 1310–1810
IRD42	2	0.41	–	080806-1	*Pomatoleios kraussii*	945 ± 84	Cal AD 1410–1580	Cal AD 1340–1660
IRD51	2	1.25	–	080806-2	*Hormomya mutabilis*	1199 ± 70	Cal AD 1230–1390	Cal AD 1170–1430
IRD61	2	1.45	–	080806-3	*Hormomya mutabilis*	2218 ± 107	Cal AD 130–390	Cal AD 0–550
IRD62	2	1.45	–	080806-4	*Pomatoleios kraussii*	2011 ± 130	Cal AD 360–650	Cal AD 150–750
IRD81	2	1.85	–	080806-5	*Pomatoleios kraussii*	1684 ± 79	Cal AD 720–900	Cal AD 670–1000
IRD82	2	1.85	–	080806-05	*Pomatoleios kraussii*	1713 ± 49	Cal AD 710–840	Cal AD 680–910
IRD91	2	2.05	–	080806-8	*Pomatoleios kraussii*	1656 ± 59	Cal AD770–920	Cal AD 710–990
IRD92	2	2.05	–	080806-9	*Pomatoleios kraussii*	1470 ± 46	Cal AD 980–1110	Cal AD 930–1170
SMD1	3	2.70	–	Beta-358327	Pholadidae	3560 ± 30	Cal BC 1427-1324	Cal BC 1466-1280
SMD2	3	2.70	–	Beta-358328	Pholadidae	3540 ± 30	Cal BC 1402-1309	Cal BC 1438-1258
SMD3	3	2.70	–	Beta-358329	Pholadidae	3530 ± 30	Cal BC 1392-1299	Cal BC 1428-1250
SMRC1	4	1.40	–	Beta-358330	*Jouannetia cumingii*	1510 ± 30	Cal AD 974–1042	Cal AD 913–1062
SMRC2	4	1.40	–	Beta-358331	*Jouannetia globulosa*	1420 ± 30	Cal AD 1048–1134	Cal AD 1025–1180
SMRC3	4	1.40	–	Beta-358332	*Zirfaea subconstricta*	1580 ± 30	Cal AD 897–985	Cal AD 839–1020
SMRC4	4	1.40	–	Beta-358333	*Zirfaea subconstricta*	1450 ± 30	Cal AD 1023–1105	Cal AD 997–1159

basis of these specimen ages (Fig. 9), boring shells at sites 3 and 4 probably experienced Uplifts 1–4, and Uplifts 2–4, respectively. Considering the uncertainties associated with the uplift estimates, we detect no significant differences in total uplift among four sites.

Ota et al. (1986) and Taguchi (1993) suggested that the southern end of Izu Peninsula had been subsiding until 3000 BP, and that three uplift events have occurred since. Our results largely support their interpretation, except for the numbers of uplift events. The occurrence of Uplift 1 (1256–950 BC) indicates when the stress field in the southern part of Izu Peninsula changed to the current stress field (Sagiya, 1999; Heki and Miyazaki, 2001; Nishimura et al., 2007). Moreover, the recurrence intervals of uplift-inducing earthquakes appear to have shortened during the past 1000 years. Active strike-slip faults are located in the study area (e.g. the Irozaki and Kamigamo faults) (Figs. 1b and 2). The AD 1974 Off-Izu Peninsula earthquake on the Irozaki Fault produced 0.1 m of uplift in the study area (Danbara and Tsuchi, 1975). Although the sense of displacement on the Kamigamo Fault is unknown, no vertical displacement has been detected. Consequently, it is thought that an unknown reversal fault(s), that caused four uplift events and crustal shortening in the study area, exists off the southern Izu Peninsula.

6.2. Origin of the scoria

To determine the origin of the scoria, the bulk rock composition was compared with published data for volcanic rocks from four active volcanoes near Shimoda including Hakone volcano (Takahashi et al., 2006), Fuji volcano (Takahashi et al., 2003), the Higashi-Izu monogenic volcanoes (Suzuki, 2000; Takahashi et al., 2002) and Izu-Oshima volcano (Fujii et al., 1988; Nakano et al., 1988; Kawanabe, 1991; Nakano and Yamamoto, 1991). The scoria was possibly derived from unknown submarine volcanoes near Shimoda, but it is difficult to determine this with any great certainty due to an absence of compositional datasets for rocks from submarine volcanoes. We therefore excluded submarine volcanoes as a candidate for the source of the scoria. Fig. 11 shows bulk Al_2O_3–FeO* compositional ranges for volcanic rocks with a bulk SiO_2 content of 54 ± 2 wt% from the four volcanic areas listed above. Volcanic rocks from Izu-Oshima volcano, located 40 km east of the study area, are distinct from the other three volcanoes because they contain higher FeO* contents and lower Al_2O_3 contents. In Fig. 11, the scoria from Shimoda overlaps with the samples from Izu-Oshima volcano. Similarly, the concentrations of other elements in the scoria are identical to those of volcanic rocks from Izu-Oshima volcano. Therefore, we conclude that the scoria was derived from Izu-Oshima volcano. This scoria is the first reported tephra from Izu-Oshima volcano found on Izu Peninsula.

Bulk-rock Al_2O_3–FeO* variations in magmas from Izu-Oshima are due mainly to the accumulation of plagioclase phenocrysts in a phenocryst-free, Al_2O_3-poor and FeO*-enriched magma (e.g., Kawanabe, 1991; Nakano and Yamamoto, 1991). The Al_2O_3 content increases with decreasing FeO* content, as the modal abundance of

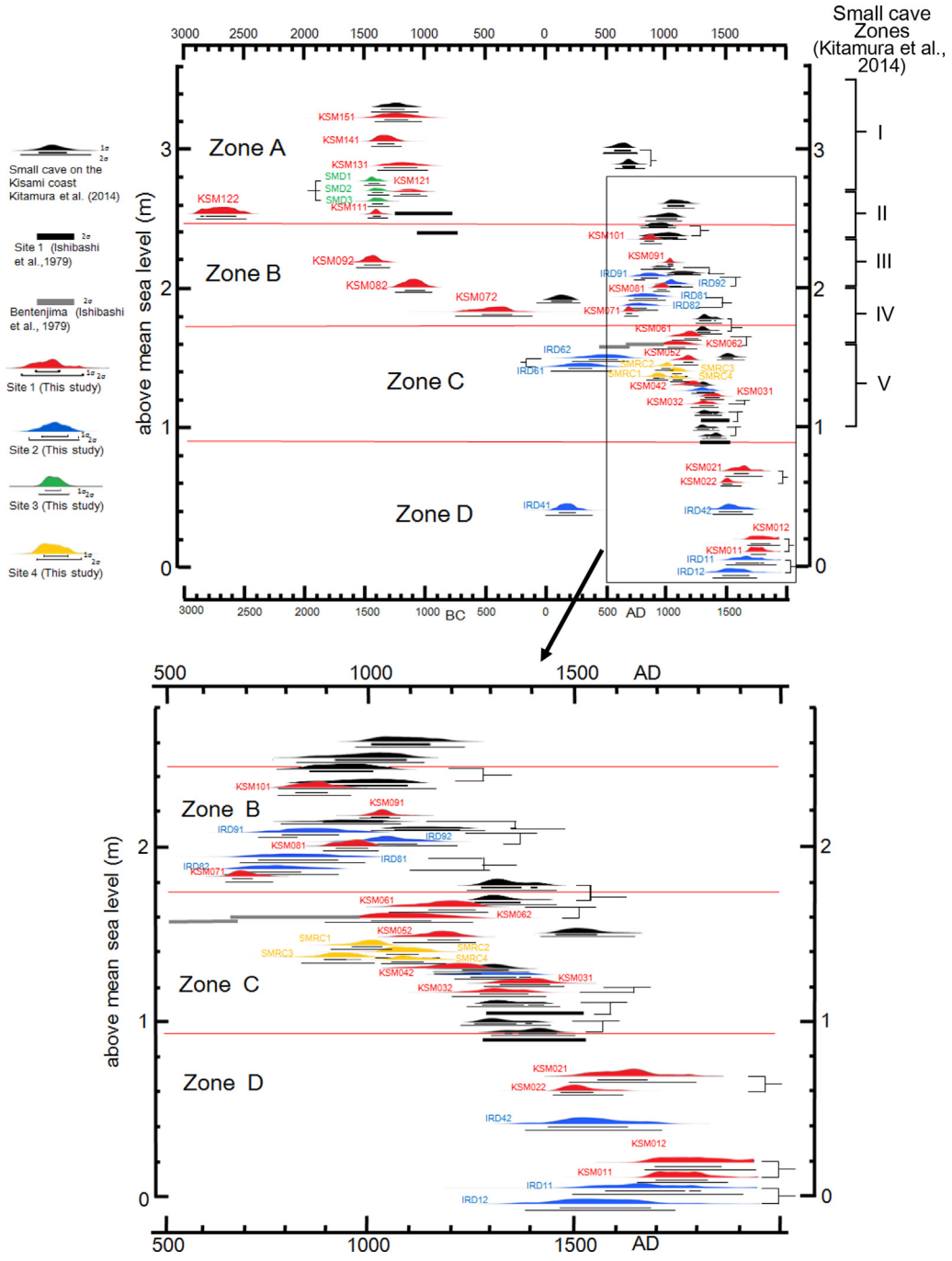

Fig. 9. Elevation distributions and ages of emerged sessile assemblages at four sites and small cave on the southern part of Izu Peninsula (Kitamura et al., 2014a).

plagioclase phenocrysts increases. The compositional and petrographic characteristics of the scoria are almost identical to the Al_2O_3-poor, FeO*-enriched end-member. Hamada et al. (2014) categorized aphiric magmas from Izu-Oshima volcano into three types: (i) the low-K subgroup, (ii) the higher-Al/Si trend of a higher-K subgroup, and (iii) the lower-Al/Si trend of a higher-K subgroup. The scoria from Shimoda is compositionally similar to the lower-Al/Si trends of a higher-K subgroup, which is formed by differentiation crystallization under conditions of relatively low pressure and low H_2O content in the melt (Hamada et al., 2014). Magmas with similar compositions to the scoria have been reported from all stratigraphic groups at Izu-Oshima volcano including the Senzu Group (>40,000 BP), the pre-caldera Older Oshima Group (40,000 to 1500 BP) and the co- and post-caldera Younger Oshima Group (<1500 BP) (e.g., Kawanabe, 1991; Hamada et al., 2014). This observation indicates that the same magma batch has fed the volcano throughout the entire eruption history of Izu-Oshima volcano.

The stratigraphic study of Uesugi et al. (1994) reported seven scoria layers at Izu-Oshima volcano, erupted at ca. 6.3–5.5 ka, indicating that Izu-Oshima volcano erupted explosively over this period. This is consistent with our conclusion that the scoria from Shimoda was derived from the Izu-Oshima volcano. However, it is difficult to compare these scoria with scoria from Shimoda because of an absence of compositional and petrographical data.

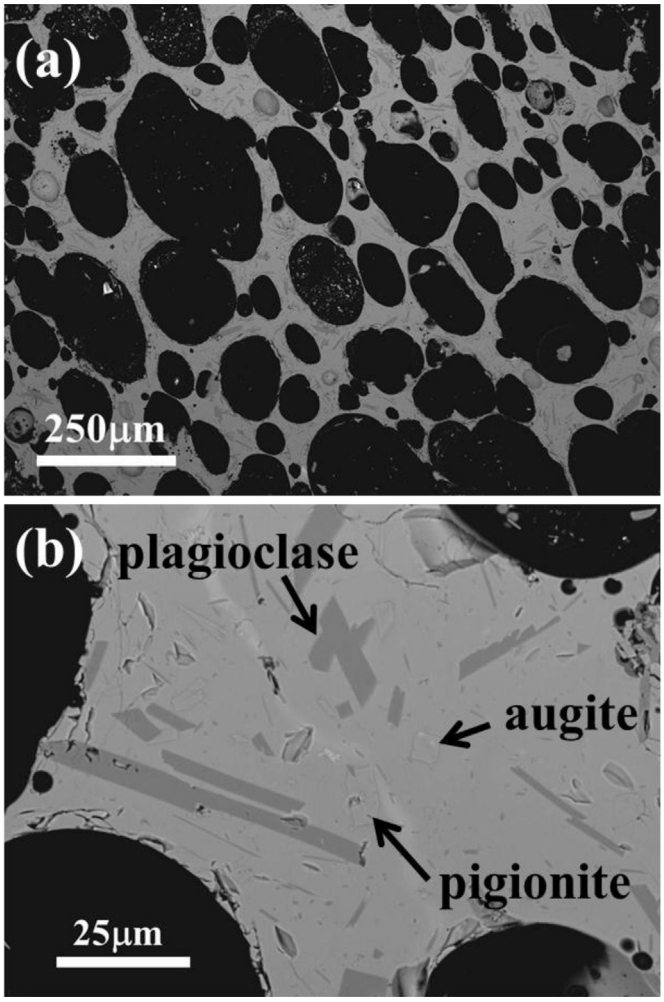

Fig. 10. Back scattered electron images of the scoria. Dark- and light-gray rectangles are plagioclase and olivine, respectively. Light-gray matrix is silicate glass and black rounded parts are bubbles filled by resin.

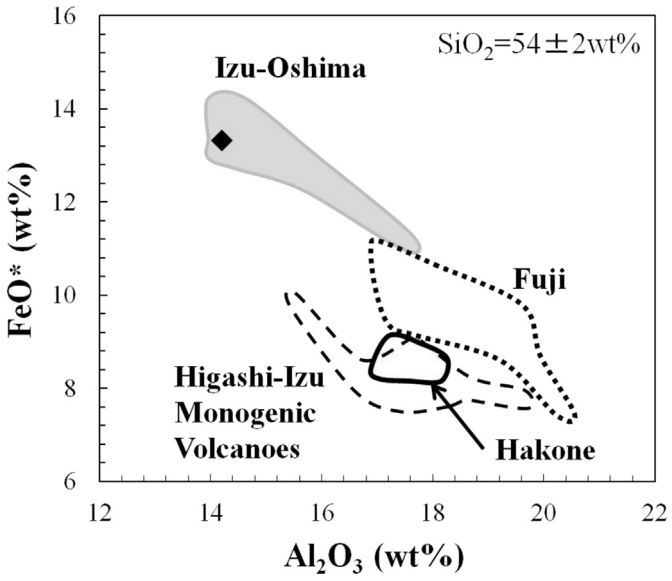

Fig. 11. Bulk FeO* content is plotted against Al_2O_3 content (diamond). Compositional ranges of volcanic rocks within bulk SiO_2 content of 54 ± 2 wt% from active volcanoes near the boring site are also shown for comparison. Volcanic rocks from Hakone volcano, Fuji volcano and Higashi-Izu monogenic volcanoes are plotted in the ranges surrounded by solid, dotted and broken curves, respectively. The gray-hatched area indicates the compositional range of volcanic rocks from Izu-Oshima volcano.

7. Conclusions

This study investigated the faunal compositions and obtained AMS ^{14}C ages of emerged sessile assemblages at four sites in the south part of Izu Peninsula, Central Japan. In addition, we examined a scoria layer that was deposited at 6940–6810 cal BP in the same part of Izu Peninsula. The results can be summarized as follows.

1. Coseismic uplifts occurred at 1256–950 BC, AD 1000–1270, AD 1430–1660, and AD 1506–1815. This indicates that the stress field in the area changed to the current condition at ca. 3100 BP, and that the recurrence intervals of uplift-inducing earthquakes have shortened over the past 1000 years. The source fault(s) of these earthquakes seems to be located off the south part of Izu Peninsula.
2. The scoria grains were probably derived from past eruption of Izu-Oshima volcano, located 40 km east of the study area, rather than a volcano on Izu Peninsular.

Table 2
Major element compositions of bulk scoria and glass (normalized to 100 wt%).

	Bulk	Glass
SiO_2	53.8	54.9
TiO_2	1.32	1.52
Al_2O_3	14.2	13.3
FeO*	13.3	13.9
MnO	0.22	0.24
MgO	4.78	4.48
CaO	9.69	9.09
Na_2O	1.98	1.91
K_2O	0.49	0.52
P_2O_5	0.13	0.23
Total	100	100
FeO*/MgO	2.79	3.10

Acknowledgements

We thank landowners in the study area for allowing us access to their land for our research activities. We also thank Dr. A. Yasuda, Ms. N. Hokanishi and Ms. N. Takagi of Earthquake Research Institute, the University of Tokyo for their technical support for EPMA analysis. We thank A. Stallard for improving the English in the manuscript. This study was funded by a grant from Strategic Funds for the Promotion of Science, Technology and the Network of Universities in Shizuoka, and Grants-in-Aid (26287126) awarded by the Japan Society for Promotion of Science. This study was conducted under permit from the Agency for Cultural Affairs, Kanto Regional the Ministry of the Environment.

References

Abe, K., Okada, M., 1993. Excitation of tsunami by a pure strike-slip earthquake—Izu Oshima Kinkai earthquake tsunami on Feb 20, 1990. Zishin 46, 25–34 (in Japanese).
Abe, T., Shirai, M., 2013. Event deposits correlated with a historical tsunami in the Edo period, on the coastal lowland of the Atsumi Peninsula, central Japan. The Quaternary Research (Daiyonki-Kenkyu) 52, 33–42.
Bronk Ramsey, C., 2009. Bayesian analysis of radiocarbon dates. Radiocarbon 51, 337–360.
Castilla, J.C., Manríquez, P.H., Camano, A., 2010. Effects of rocky shore coseismic uplift and the 2010 Chilean mega-earthquake on intertidal biomarker species. Marine Ecology – Progress Series 418, 17–23.

Danbara, T., Tsuchi, R., 1975. Crustal movements in the southern Izu Peninsula. Geoscience Reports of Shizuoka University 1, 27–30 (in Japanese).
Danhara, T., Yamashita, T., Iwano, H., Kasuya, M., 1992. An improved system for measuring refractive index using thermal immersion method. Quaternary International 13/14, 89–91.
Fujii, T., Aramaki, S., Kaneko, T., Ozawa, K., Kawanabe, Y., Fukuoka, T., 1988. Petrology of the lava and ejecta of the November, 1986 eruption of Izu-Oshima volcano. Bulletin of the Volcanological Society of Japan 33, S234–S254 (in Japanese with English abstract).
Fujiwara, O., Sato, Y., Ono, E., 2013. Researches on tsunami deposits using sediment cores: 3.4 ka tsunami deposit in the Rokken-gawa Lowland near Lake Hamana, Pacific coast of Central Japan. Journal of Geography (Chigaku Zasshi) 122, 308–322 (in Japanese with English abstract).
Fukutomi, K., 1935. Crustal movements of Izu Peninsula, Central Japan, based on historical documents and oral traditions. Zisin (Journal of the Seismological Society of Japan) 7, 1–15 (in Japanese).
Hamada, M., Okayama, Y., Kaneko, T., Yasuda, A., Fujii, T., 2014. Polybaric crystallization differentiation of H_2O-saturated island arc low-K tholeiite magmas: a case study of the Izu- Oshima volcano in the Izu arc. Earth, Planets and Space 66, 15.
Hamuro, K., 1977. ^{14}C ages of Chikubo central cone scoria fall, kawagodaira pyroclastic flow, Omuroyama-Amagi lateral volcano groups, izu Peninsula. Bulletin of the Volcanological Society of Japan. Second series 22 (4), 277–278 (in Japanese).
Hamuro, K., 1985. Petrology of the Higashi-Izu monogenetic volcano group. Bulletin Earthquake Research Institute, University of Tokyo 60, 335–400.
Hatori, T., 1976. Documents of tsunami and crustal deformation in Tokai district associated with the Ansei earthquake of Dec. 23, 1854. Bulletin of the Earthquake Research Institute, University of Tokyo 51, 13–28 (in Japanese with English abstract).
Heki, K., Miyazaki, S., 2001. Plate convergence and long-term crustal deformation in Central Japan. Geophysical Research Letters 28, 2313–2316.
Ikeya, N., Wada, H., Akutsu, H., Takahashi, M., 1990. Origin and sedimentary history of Hamana-ko Bay, Pacific coast of central Japan. The Memoirs of the Geological Society of Japan 36, 129–150 (in Japanese with English abstract).
Iryu, Y., Maemoku, H., Yamada, T., Maeda, Y., 2009. Limestones as a paleobathymete for reconstructing past seismic activities: Muroto-misaki, Shikoku, southwestern Japan. Global and Planetary Change 66, 52–64.
Ishibashi, K., Ota, Y., Matsuda, T., 1979. Radiocarbon ages of raised shell beds at the southern tip of Izu Peninsula, central Japan. Zisin (Journal of the Seismological Society of Japan) 32, 105–107 (in Japanese).
Kawanabe, Y., 1991. Petrological evolution of Izu Oshima volcano. Bulletin of the Volcanological Society of Japan 36, 281–296 (in Japanese with English abstract).
Kitamura, A., Fujiwara, O., Shinohara, K., Akaike, S., Masuda, T., Ogura, K., Urano, Y., Kobayashi, K., Tamaki, C., Mori, H., 2013a. Identifying possible tsunami deposits on the Shizuoka Plain, Japan and their correlation with earthquake activity over the past 4000 years. The Holocene 23, 1682–1696.
Kitamura, A., Itasaka, K., Ogura, K., Ohashi, Y., Saito, A., Uchida, J., Nara, M., 2013b. Preliminary study on tsunami deposits from the coastal lowland of Minami Izu, Shizuoka Prefecture. Geoscience Reports of Shizuoka University 40, 1–12 (in Japanese with English abstract).
Kitamura, A., Kobayashi, K., 2014a. Geologic evidence for prehistoric tsunamis and coseismic uplift during the AD 1854 Ansei-Tokai earthquake in Holocene sediments on the Shimizu Plain, central Japan. The Holocene 24, 814–827.
Kitamura, A., Kobayashi, K., 2014b. Geologic record of middle–late Holocene paleotsunamis and paleo-earthquakes on the Shizuoka Plain and coastal lowland of the southern Izu Peninsula, central Japan. Journal of Geography (Chigaku Zasshi) 122, 813–834 (in Japanese with English abstract).
Kitamura, A., Koyama, M., Itasaka, K., Miyairi, Y., Mori, H., 2014a. Abrupt Late Holocene uplifts of the southern Izu Peninsula, central Japan: evidence from emerged marine sessile assemblages. Island Arc 23, 51–61.
Kitamura, A., Ohashi, Y., Miyairi, Y., Yokoyama, Y., Yamaguchi, T., 2014b. Discovery of a tsunami boulder along the coast at Shimoda, Shizuoka, Central Japan. The Quaternary Research (Daiyonki-Kenkyu) 53, 259–264 (in Japanese with English abstract).
Koyama, M., Umino, S., 1991. Why does the Higashi-Izu monogenetic volcano group exist in the Izu Peninsula?: relationships between late Quaternary volcanism and tectonics in the northern tip of the Izu-Bonin Arc. Journal of Physics of the Earth 39, 391–420.
Le Mitre, R.W., 2002. Igneous Rocks – a Classification and Glossary of Terms. Recommendations of the IUGS Subcommision on the Systematics of Igneous Rocks, second ed. Cambridge University Press, Cambridge.
Melnick, D., Cisternas, M., Moreno, M., Norambuena, R., 2012. Estimating coseismic coastal uplift with an intertidal mussel: calibration for the 2010 Maule Chile earthquake ($Mw = 8.8$). Quaternary Science Reviews 42, 29–42.
Murai, I., Kaneko, N., 1974. The Izu-Hanto-oki earthquake of 1974 and the earthquake faults, especially, the relationships between the earthquake faults, the active faults, and the fracture systems in the earthquake area. Special Bulletin of the Earthquake Research Institute, University of Tokyo 14, 159–203 (in Japanese and English).
Nakamura, K., Shimazaki, K., 1981. Sagami and Suruga Troughs and subduction of plates. Science (Kagaku), Iwanami Shoten 51, 490–498 (in Japanese).
Nakanishi, A., Shinohara, H., Hino, R., Kodaira, S., Kanazawa, T., Shimamura, H., 1994. Detailed subduction structure of the Philippine Sea plate off Tokai district deduced by airgun-ocean bottom seismograph profilling –crustal structure of the Zenisu Ridge and the eastern Nankai Trough–. Zisin (Journal of the Seismological Society of Japan) 47, 311–331 (in Japanese).
Nakano, S., Yamamoto, T., 1991. Chemical variations of magmas at Izu-Oshima volcano, Japan: plagioclase-controlled and differentiated magmas. Bulletin of Volcanology 53, 112–120.
Nakano, S., Yamamoto, T., Takada, A., Soya, T., 1988. Chemical variation of fissure eruption products at post-caldera Y5 stage of Izu-Oshima volcano. Bulletin of the Volcanological Society of Japan 33, 31–35 (in Japanese with English abstract).
Nishimura, T., Sagiya, T., Stein, R.S., 2007. Crustal block kinematics and seismic potential of the northernmost Philippine Sea plate and Izu microplate, central Japan, inferred from GPS and leveling data. Journal of Geophysical Research: Solid Earth (1978–2012) 112 (B5). http://dx.doi.org/10.1029/2005JB004102.
Notsu, K., Sohrin, R., Wada, H., Tsuboi, T., Sumino, H., Mori, T., Tsunogai, U., Hernández, P.A., Suzuki, Y., Ikuta, R., Oorui, K., Koyama, M., Masuda, T., Fujii, N., 2014. Leakage of magmatic–hydrothermal volatiles from a crater bottom formed by a submarine eruption in 1989 at Teishi Knoll, Japan. Journal of Volcanology and Geothermal Research 270, 90–98.
Oshima, S., Hydrographic Department Survey Team of Earthquake and Volcano off Ito, Ossaka, J., Kudo, K., Sakaue, M., 1990. Submarine volcanic eruption of Teishi Knoll off eastern part of Izu Peninsula. Report Hydrographic Research 26, 1–43 (in Japanese with English abstract).
Oshima, S., Tsuchide, M., Kato, S., Okubo, S., Watanabe, K., Kudo, K., Ossaaka, J., 1991. Birth of a submarine volcano "Teishi Knoll". Journal of Physics of the Earth 39, 1–19.
Ota, Y., Ishibashi, K., Matsushima, Y., Matsuda, T., Miyoshi, M., Kashima, K., Matsubara, A., 1986. Holocene relative sea-level change in the southern pert of Izu Peninsula, central Japan; Data from subsurface investigation. The Quaternary Research (Daiyonki-Kenkyu) 25, 203–223 (in Japanese with English abstract).
Reimer, P.J., Bard, E., Bayliss, A., Beck, J.W., Blackwell, P.G., Bronk Ramsey, C., Buck, C.E., Edwards, R.L., Friedrich, M., Grootes, P.M., Guilderson, T.P., Haflidason, H., Hajdas, I., Hatté, C., Heaton, T.J., Hoffmann, D.L., Hogg, A.G., Hughen, K.A., Kaiser, K.F., Kromer, B., Manning, S.W., Niu, M., Reimer, R.W., Richards, D.A., Scott, M.E., Southon, J.R., Turney, C.S.M., van der Plicht, J., 2013. IntCal13 and Marine13 radiocarbon age calibration curves 0–50,000 yr cal BP. Radiocarbon 55, 1869–1887.
Sagiya, T., 1999. Interplate coupling in the Tokai district, central Japan, deduced from continuous GPS data. Geophysical Research Letters 26, 2315–2318.
Sano, T., 2003. Determination of major and trace element contents in igneous rocks by X–ray fluorescence spectrometer analysis. Bulletin of Fuji–Tokoha University of the years 2002–2003 2, 43–59 (in Japanese with English abstract).
Scicchitano, G., Spampinato, C.R., Ferranti, L., Antonioli, F., Monaco, C., Capano, M., Lubritto, C., 2011. Uplifted Holocene shorelines at Capo Milazzo (NE Sicily, Italy): evidence of co-seismic and steady-state deformation. Quaternary International 232, 201–213.
Shimada, S., 2000. Eruption of the Amagi-Kawagodaira Volcano and paleoenvironments in the late and latest Jomon periods around Izu Peninsula. The Quaternary Research (Daiyonki-Kenkyu) 39, 151–164 (in Japanese with English abstract).
Shishikura, M., Echigo, T., Maemoku, H., Ishiyama, T., 2008. Height and ages of uplifted sessile assemblage distributed along the southern coast of the Kii Peninsula, south-central Japan –Reconstruction of multi-segment earthquake history along the Nankai Trough–. Annual Report on Active Fault and Paleoearthquake Researches 8, 187–202 (in Japanese with English abstract).
Smith, V.C., Staff, R.A., Blockley, S.P.E., Ramsey, C.B., Nakagawa, T., Mark, D.F., Takemura, K., Danhara, T., 2013. Identification and correlation of visible tephras in the Lake Suigetsu SG06 sedimentary archive, Japan: chronostratigraphic markers for synchronizing of east Asian/west Pacific palaeoclimatic records across the last 150 ka. Quaternary Science Reviews 67, 121–137.
Somervill, P., 1978. The accommodation of plate collision by deformation in the Izu block, Japan. Bulletin Earthquake Research Institute, University of Tokyo 53, 629–648.
Sugimura, A., 1972. Plate boundary around Japan. Science (Kagaku), Iwanami Shoten 42, 192–202 (in Japanese).
Suzuki, Y., 2000. Petrogenesis of felsic magma in Higashi-Izu monogenic volcano group. Bulletin of the Volcanological Society of Japan 45, 149–171 (in Japanese with English abstract).
Taguchi, K., 1993. Holocene relative sea-level change in Izu Peninsula, Central Japan. The Quaternary Research (Daiyonki-Kenkyu) 32, 13–29 (in Japanese with English abstract).
Takahashi, M., Kikuchi, K., Urushihata, T., Aramaki, S., Hamuro, K., 2002. Incompatible element chemistry for basaltic rocks in the Higashi-Izu monogenic volcano group. Proceedings of the Institute of Natural Sciences, Nihon University 37, 119–134.
Takahashi, M., Kominami, M., Nemoto, Y., Hasegawa, Y., Nagai, T., Tanaka, H., Bishi, N., Yasui, M., 2003. Whole-rock chemistry for eruptive products of Fuji volcano, central Japan: summary of analytical data of 857 samples. Proceedings of the Institute of Natural Sciences, Nihon University 38, 117–166.
Takahashi, M., Naito, S., Nakamura, N., Nagai, M., 2006. Whole-rock chemistry for eruptive products of older and younger central cone in Hakone volcano, central Japan. Proceedings of the Institute of Natural Sciences, Nihon University 41, 151–186.

Tani, S., Kitagawa, H., Hong, W., Park, J.H., Sung, K.S., Park, G., 2013. Age determination of the Kawagodaira volcanic eruption in Japan by ^{14}C wiggle-matching. Radiocarbon 55, 748–752.
Uesugi, Y., Shinkawa, K., Kigoshi, K., 1994. Tephras outcropping along the so-called "Chisoh-setudanmen" roadcuts, Sembazaki, Izu-Oshima Volcano, Central Japan: Standard tephra columns. The Quaternary Research (Daiyonki-Kenkyu) 33, 165–187.
Usami, T., 1975. Descriptive Catalogue of Disaster Earthquakes in Japan. University of Tokyo Press, Tokyo, p. 327 (in Japanese).
Yamaguchi, T., Hisatsune, Y., 2006. Taxonomy and identification of Japanese barnacles. Sessile Organisms 23, 1–15 (in Japanese).
Yoneda, M., Kitagawa, H., van der Plicht, J., Uchida, M., Tanaka, A., Uehiro, T., Shibata, Y., Morita, M., Ohno, T., 2000. Pre-bomb marine reservoir ages in the western north Pacific: preliminary result on Kyoto University collection. Nuclear Instruments and Methods in Physics Research B 172, 377–381.